Ultrasound in Med. & Biol. Vol. 16, No. 3, pp. 247–260, 1990
Printed in the U.S.A.

0301-5629/90 $3.00 + .00

●*Original Contribution*

COMPUTER EVALUATION OF DOPPLER SPECTRAL ENVELOPE AREA IN PATIENTS HAVING A VALVULAR AORTIC STENOSIS

GUY CLOUTIER[†], FRANÇOIS LEMIRE[‡], LOUIS-GILLES DURAND[†], YVES LATOUR[‡] and YVES E. LANGLOIS[§]

[†]Biomedical Engineering Laboratory, Clinical Research Institute of Montreal and Biomedical Engineering Institute, Ecole Polytechnique, Université de Montréal, Québec, Canada.
[‡]Cardiology Division, Hôtel-Dieu de Montréal Hospital, Université de Montréal, Québec, Canada.
[§]Cardiovascular Surgery Division, Hôtel-Dieu de Montréal Hospital, Université de Montréal, Québec, Canada.

(*Received* 12 *April* 1989; *in final form* 13 *September* 1989)

Abstract—The reliability of three algorithms to estimate the maximal and minimal frequency contours of Doppler spectrograms was evaluated in a group of 48 patients. Two algorithms had previously been used in the literature. These are the Modified Threshold Crossing Method and the Hybrid method. The third algorithm is new and is the Maximal Background Noise Threshold Crossing Method. A new approach was also proposed in the present study to estimate the background noise level of Doppler spectrograms. This level was used as a threshold in the computation of the spectral envelopes. Two diagnostic spectral parameters (the spectral envelope area and the systolic velocity integral) extracted from Doppler spectrograms recorded in the left ventricular outflow tract were also evaluated and tested to discriminate between 23 patients having no aortic pressure gradient and 25 patients with a stenotic aortic valve. Results describe the influence of the threshold level used in the Modified Threshold Crossing Method and the Hybrid method on the variability of the spectral contours. It is clearly demonstrated that the variability of minimal frequency contours is higher than that of maximal frequency contours. All three algorithms provided similar diagnostic performances with the spectral envelope area (71% to 73% of correct classifications) while the Maximal Background Noise Threshold Crossing Method and the Hybrid method provided the best results for the systolic velocity integral (69% of correct classifications). Because the systolic velocity integral combined with the continuity equation is used in the literature to evaluate noninvasively the aortic valve area, these results suggest the use of the spectral envelope area instead of the systolic velocity integral.

Key Words: **Maximal frequency contour, Minimal frequency contour, Spectral envelope area, Systolic velocity integral, Continuity equation, Background noise level estimation, Doppler ultrasound spectrum, Digital signal processing.**

1. INTRODUCTION

Recent advances in clinical Doppler echocardiography combined with two-dimensional imaging have increased the accuracy of the noninvasive assessment of valvular aortic stenosis. Using continuous-wave (CW) Doppler echocardiography, patients with aortic valve stenosis can be identified by the detection of high flow velocities across the stenotic valve during systole. More precisely, maximal and mean pressure gradients can be estimated by using the modified Bernoulli equation (Zoghbi 1988; Panidis et al. 1986; Currie et al. 1985; Berger et al. 1984; Stamm and Martin 1983; Hatle et al. 1980). Moreover, the application of the continuity equation to Doppler recordings, combined with echocardiographic imaging, has yielded accurate measurements of aortic valve area (Zoghbi 1988; Oh et al. 1988; Otto et al. 1986; Zoghbi et al. 1986). Recently, the aortic jet width estimated by color Doppler imaging system has provided another approach to assess the severity of valvular aortic stenosis (Fan et al. 1988). Despite these promising clinical studies, several steps still have to be done in digital signal processing of Doppler information to simplify and reduce operators' manipulations, and to provide consistent performance of these evaluation methods.

In 1982, Cannon et al. evaluated the reliability of a new index, the spectral envelope area (SEA), to detect blood flow disturbance induced by valvular

Correspondence, reprint, and software requests should be addressed to Guy Cloutier, Clinical Research Institute of Montreal, 110 avenue des Pins ouest, Montréal, Québec, Canada, H2W 1R7. The software programs are written in C language and run on a compatible IBM-386 system. At least 1 Mbyte of expended memory is needed. A small charge might be incurred to cover the cost of computer diskettes and expedition.

aortic stenosis. The clinical usefulness of this parameter was confirmed by Richards et al. (1983). In this study of Richards et al., SEA was evaluated in patients with aortic stenosis, aortic regurgitation, mitral stenosis and mitral regurgitation, and was shown to be statistically different ($p < 0.01$) from the values obtained in a group of patients having no valvular pathology. In 1985, Cannon et al. tested the diagnostic value of SEA in a pulsatile flow model. Good correlations were found between this index and both the mean systolic pressure gradient and the aortic valve area of the model. In all these studies (Cannon et al. 1982; 1985; Richards et al. 1983), SEA was evaluated graphically by planimetry and was defined as the area between maximal and minimal frequency contours of Doppler spectrograms. Moreover, SEA was obtained by using signals recorded downstream from the aortic valve and was computed only in systole for patients with aortic valve stenosis.

The "systolic velocity integral" (also labeled as the "time-velocity integral") of pulsed-wave (PW) Doppler spectrograms recorded below the aortic valve is a parameter used in the continuity equation to evaluate the aortic valve area (Oh et al. 1988; Otto et al. 1986; Zoghbi et al. 1986). Recently, Penn and Dumesnil (1988) proposed the evaluation of the maximal aortic pressure gradient from pulsed-wave Doppler tracings recorded in the left ventricular outflow tract. These works suggested that information concerning the severity of aortic valve stenosis should be obtained from maximal and minimal frequency contours of Doppler spectrograms recorded *below* the aortic valve.

The visual localization of the frequency contours of the Doppler spectrogram is relatively easy because the eyes act like a filter which help in discriminating between the Doppler signal and the background noise. A computer based algorithm designed to perform this task should have the capability to determine the best threshold between the signal and the background noise. Because cardiac Doppler spectrograms are characterized by a low signal-to-noise (S/N) ratio and because the amplitude of the background noise varies from one patient to another and from one intracardiac sample site to another, the computer evaluation of SEA is not straightforward. The proposed algorithm must be adaptive to the level of the background noise.

Theoretical bases

Different computer based algorithms were proposed to estimate the maximal frequency contour of Doppler spectrograms. Harward et al. (1987) evaluated the clinical usefulness of maximal frequencies computed by finding the 15% amplitude level of the dominant frequency peaks. The discriminant property of maximal frequencies to detect aortoiliac artery disease showed significant overlap between the various disease groups. D'Alessio (1985) introduced a more objective algorithm which was based on the statistical characteristics of Doppler spectrograms obtained by using the Fast-Fourier Transform with rectangular window. The suggestion of using an adaptive algorithm with the level of the S/N ratio of the Doppler signal was first introduced in this work. Recently, Mo et al. (1988) evaluated this algorithm and proposed other adaptive methods to compute maximal Doppler frequency contours. Based on a simulation of single-cycle continuous-wave carotid Doppler spectrogram, the Modified Threshold Crossing and the Hybrid methods appeared to be the best algorithms. These will be described in the Method section.

As mentioned previously, the most important characteristic of a good frequency contour estimator is its capability to adjust with the level of the background noise. The noise level was often estimated by computing the amplitude of the Doppler spectrogram over a region where blood flow signal is not present. For example, the approach used by D'Alessio (1985) consisted in evaluating the average amplitude of 20 to 30 frequency samples localized at the tail of each spectrum of the Doppler spectrogram as an estimate of the background noise. One major problem with this approach is the possibility that significant blood flow signals exist in the selected tail portion of each spectrum. Another approach proposed by Heringa et al. (1988) consisted in estimating the noise level by taking the average amplitude of frequency samples included in the lower part of the distribution function of Doppler spectrograms computed over several cardiac cycles. In their algorithm, the background noise level was estimated by assuming that the lower 33% of the distribution function of each spectrum contains noise only. One limitation of this algorithm is the arbitrary selection of the 33% threshold. The problem of estimating the level of the background noise in practical situations was not investigated by Mo et al. (1988). Indeed, they circumvented this problem by limiting the simulation of blood flow Doppler signals to 7 kHz in their study. The value of the background noise was then estimated by averaging the amplitude of the samples of each spectrum localized above 7 kHz.

Outline of the study

As emphasized previously, the problem of estimating the level of the background noise of Doppler spectrograms in practical situations is not straightforward. In the present study, a new approach is proposed and used to tune the adaptive frequency contour estimators. A statistical procedure has been integrated to the method to eliminate frequency samples associated with blood flow in the computation of the background noise level. The algorithm has been applied to pulsed-wave Doppler signals but it is also proposed that the algorithm could be used for continuous-wave analysis of cardiac Doppler signals.

Using this new approach, the reliability of three different algorithms to estimate the spectral envelope area and the systolic velocity integral of Doppler spectrograms has been evaluated in 48 patients having a stenotic or nonstenotic aortic valve. Two of the three algorithms tested are based on the Modified Threshold Crossing and the Hybrid methods proposed by Mo et al. (1988) which have been adapted to evaluate both maximal and minimal frequency contours of the spectrograms. The third algorithm is new and is named Maximal Background Noise Threshold Crossing Method. Special care has been taken in all algorithms to reduce the influence of high amplitude low-frequency vibrations in the computation of the minimal frequency contours.

2. MATERIALS AND METHODS

Patient selection and data acquisition

A group of 48 patients referred to the Hôtel-Dieu de Montréal Hospital for a catheterization examination was included in the present study. Twenty-three patients had no aortic pressure gradient and 25 had aortic valve stenosis. The patient population having no aortic pressure gradient was composed of patients referred for pure aortic regurgitation or coronary artery disease.

Measurements of transvalvular maximal and mean pressure gradients were based on retrograde left-heart catheterization. Both pull-back and simultaneous recording methods were used to estimate aortic pressure gradients (Grossman 1986). Supravalvular aortography was done in all patients to assess the severity of possible aortic regurgitation on a four degree scale (minimal, mild, moderate, and severe). Visualization of the regurgitant jet by cineangiography from a left anterior oblique projection served to estimate the severity of the valvular insufficiency according to the criteria proposed by Grossman (1986). For all patients with suspected aortic valve disease, the cardiac output was measured by the dye-dilution technique.

A Doppler investigation was performed generally within 1 day of the catheterization examination. During this investigation, the following signals were recorded on a 4-channel tape recorder for a period of approximately 30 seconds: the direct and quadrature Doppler signals, the phonocardiogram (PCG) recorded from the second right intercostal space (aortic area) and the electrocardiogram (ECG). A TASCAM 22-4 tape recorder having a dynamic range of 40 dB was modified to include two frequency modulated channels. Both Doppler signals were recorded in direct mode while both PCG and ECG signals were recorded in frequency modulation mode. At a speed of 7.5 inches per second, the frequency response of the direct channels is uniform (−3 dB) between 50 and 20,000 Hz and that of the frequency modulated channels is uniform (−3 dB) between 0 and 2500 Hz.

Both ECG and PCG signals were used to synchronize the detection of the systolic phase of the Doppler signals. The systolic period was defined as the interval between the R-wave of the ECG and the beginning of the second heart sound of the PCG. The evaluation of the spectral parameters and the estimation of the variability of minimal and maximal frequency contours of Doppler spectrograms were limited to the systolic period.

A duplex ultrasound scanner system (Advanced Technological Laboratory, Ultramark 8) using a pulsed-wave probe operating at 3 MHz was used to record the Doppler blood flow signals at the midpoint of the left ventricular outflow tract, approximately 1 cm below the aortic valve. The apical echocardiographic view was used to obtain those signals. For each recording, the wall filter was set at 200 or 400 Hz to reduce the high amplitude low-frequency signals. This procedure allows the reduction of the dynamic range of the Doppler signals which results in a better visual detection of the envelope. The High-Pulse-Repetition-Frequency (HPRF) mode was selected if frequency aliasing occurred. The HPRF mode was not used if additional sample volumes were in a blood flow region.

The selection of the dimension of the sample volume influences the spectral broadening of Doppler spectrograms as reported by van Merode et al. (1983). In this study, visual grading of cervical carotid artery narrowing from the degree of spectral broadening showed better results when using a small sample volume. The same group proposed methods to evaluate the dimension of the sample volume on the lateral and axial directions (Hoeks et al. 1984). These methods were not applied in the present study because of the noncommercial availability of the equipment required. The axial dimension of the sample volume was set at 1.5 mm for all analyses, as stated by the manufacturer's specifications. The dimension of the sample volume on the lateral axis was not estimated.

Spectral analysis

During playback, the ECG, PCG, and PW Doppler signals were digitized for 15 seconds with 12-bit resolution at sampling rates of 0.2, 2, and 20 kHz, respectively. Prior to digitization, the Doppler signals were low-pass filtered at 9 kHz with two eight-order filters (−48 dB/octave). Before computing Doppler spectrograms, a *QRS* detection algorithm based on a correlation technique was used to locate the beginning of each cardiac cycle. The mean *RR* interval and its standard deviation were then computed for each patient over the digitized period of 15 seconds. The ratio of the standard deviation to the mean *RR* interval was also computed for each patient to assess the variability of the heart cycle durations. Averaged value of the mean *RR* interval of the 48 patients was 898 ± 156 ms (mean heart rate of 67 bpm). The average value of the variability of the *RR* intervals computed over the 48 patients was 3.6% (range of 0.4% to 32.4%). For each patient, by selecting consecutively each cardiac cycle, only those having a duration within ±10% of its mean *RR* interval were kept for spectral analysis.

A Hanning window of 10 ms was applied to the Doppler signals and a complex Fast-Fourier Transformation (FFT) was computed to obtain a 256-sample power spectrum. The Hanning window was then slid over the entire cardiac cycle and an FFT computed at each increment of 5 ms to produce a power spectrogram of the Doppler signals (Portnoff 1980). An ensemble average of the power spectrograms computed on 5 cardiac cycles was taken to reduce the variability of the spectral representation. The temporal reference of the *QRS* complex of the ECG served to align the spectrograms. The averaging process was limited to the interval corresponding to the duration of the minimal heart cycle of the patient. Because only the cardiac cycles having a duration within ±10% of the mean *RR* interval were analyzed, the maximal duration of the rejected diastolic portion of the spectrograms was then limited to 20% of the mean *RR* interval. A typical average power Doppler spectrogram of a patient with a stenotic aortic heart valve is presented in Fig. 1.

Background noise level estimation

In the present study, as suggested by D'Alessio (1985) and Mo et al. (1988), it is assumed that the background noise is a white Gaussian process with constant spectral density N_0. We also assume that the background noise of Doppler spectrograms is time invariant. These assumptions are used to justify the method proposed to estimate the background noise.

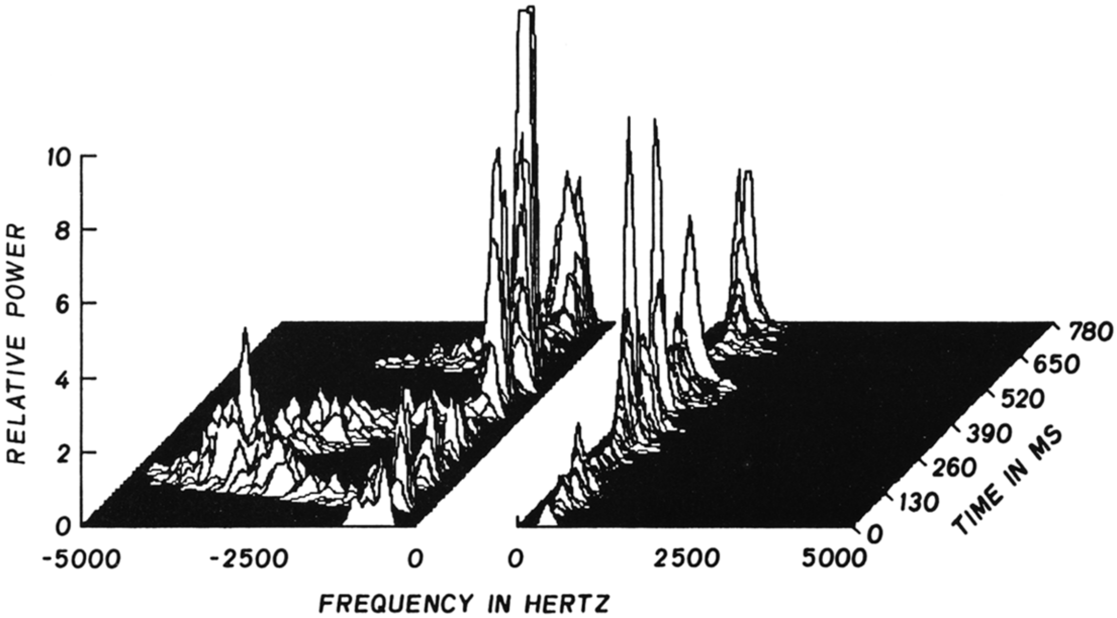

Fig. 1. Typical average power Doppler spectrogram of a patient with a stenotic aortic heart valve. This spectrogram is characterized by the presence of high amplitude low-frequency vibrations. The pulsed-wave Doppler signals were recorded at the midpoint of the left ventricular outflow tract, approximately 1 cm below the aortic valve. The negative frequencies of the spectrogram represent blood flow moving toward the aorta while the positive frequencies correspond to blood flow moving backward to the left ventricle.

A first estimate of N_0 was obtained by averaging samples of all spectra of the average Doppler spectrogram localized at ± the Pulse-Repetition-Frequency (PRF) divided by two, at +PRF/2 minus one sample and at −PRF/2 plus one sample. These frequency samples were also used to describe the statistical distribution of the background noise. The upper frequency limits of ±PRF/2 was chosen because low-pass filtering was performed by the Ultramark 8 Ultrasound system above these frequencies. In the specific cases where the HPRF mode was used, samples localized close to the extinction frequency of the anti-aliasing low-pass filter (*i.e.*, 9 kHz) were used if HPRF/2 exceeded this value.

Because frequency aliasing often occurs in PW cardiac Doppler analysis, special attention was taken to ensure that no Doppler blood flow velocity component was found close to ±PRF/2. The following procedure was used to eliminate samples originating from frequency aliasing in the computation of $\hat{N}_0$ (estimated value of N_0). First, visual inspection of each average spectrogram of the 48 patients was performed to identify spectrograms showing frequency aliasing. Secondly, values of the coefficient of skewness and of the coefficient of variation (in percent) of the statistical distribution of the background noise of each average spectrogram having no frequency aliasing were computed and averaged. The mean values of these parameters were then used as *a priori* information to determine the reference threshold needed to reject any blood flow velocity component as described in the following paragraph.

Samples with higher amplitude, which probably resulted from frequency aliasing, were successively eliminated one by one from the statistical distribution of the background noise of the 48 patients studied and the coefficient of skewness and the coefficient of variation recomputed at each step. This iterative procedure was stopped when the coefficient of skewness and the coefficient of variation reached the preselected reference thresholds described previously. For patients having values below these thresholds, no sample was eliminated from the statistical distribution function. The final estimate of N_0 was obtained by averaging the amplitude of the samples of the residual statistical distribution function of the background noise.

Spectral envelope determination

Three computer based algorithms were evaluated in the present study to estimate the spectral envelope area (SEA) and the systolic velocity integral (SVI) of average Doppler spectrograms. The first algorithm was based on the Modified Threshold Crossing Method (MTCM) and the second on the Hybrid method proposed by Mo et al. (1988). Both algorithms were improved to estimate maximal and minimal frequency contours. The third algorithm is a variant of the Modified Threshold Crossing Method that we have named the Maximal Background Noise Threshold Crossing Method (MBNTCM). For all algorithms, the quantification of SEA (in kHz) was obtained by adding, over the systolic period, the difference between the estimated maximal ($\hat{F}$max) and minimal ($\hat{F}$min) frequencies of the envelopes. The systolic velocity integral expressed in kHz was computed by adding, over the systolic period, the estimated maximal frequencies of the envelopes. A review of the fundamental bases of these algorithms is presented next.

The Threshold Crossing and the Hybrid methods. The Modified Threshold Crossing Method used by Mo et al. (1988) is based on the following algorithm: Starting from the noise end of each power spectrum, spectral samples in successive frequency bins are compared to a threshold level. If, in a sequence of successive bins there are at least 2 bins that exceed the threshold, then the maximal frequency of the spectrum is taken to be the highest bin frequency in that sequence. Based on their simulation (Mo et al. 1988), the optimal threshold should be selected at 8 $\hat{N}_0$ for a S/N ratio of the CW Doppler spectrogram ranging between 5 and 13 dB and at 11 $\hat{N}_0$ for a S/N ratio ranging between 13 and 20 dB.

The Hybrid method proposed by Mo et al. (1988) consists of finding the intersection between a straight line, having a slope proportional to $\hat{N}_0$, and the integrated Doppler power spectrum $I(f)$ of the spectrogram. To estimate the maximal frequency contour of the negative portion of the Doppler spectrograms with this algorithm, the straight line passes through the point (−PRF/2, I(−PRF/2)) as described in the following equation:

$$I(\hat{F}\text{max}) = I(-\text{PRF}/2) - K\hat{N}_0(\text{PRF}/2 + \hat{F}\text{max}), \quad (1)$$

where K represents the constant of proportionality of the slope and $\hat{F}$max the estimated maximal frequency of the spectrum. The estimate of Fmax is given by the lowest frequency (in absolute value) that satisfies eqn (1). According to Mo et al. (1988), parameter K should be 3 for a S/N ratio of the CW Doppler spectrogram ranging between 5 and 13 dB, and 4.5 for a S/N ratio ranging between 13 and 20 dB.

Improvements of the Threshold Crossing methods. The following approach is proposed to compute simultaneously minimal and maximal fre-

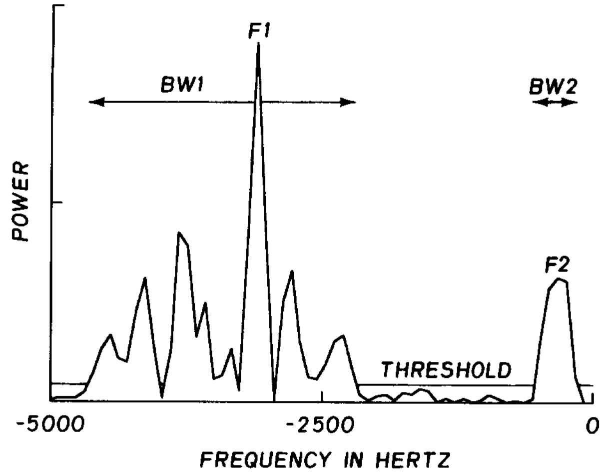

Fig. 2. Typical power Doppler spectrum characterized by the presence of a high amplitude low-frequency vibration. BW1 and BW2 are associated to the bandwidth of the dominant (F1) and second dominant frequency peaks (F2).

quency contours. Figure 2 helps in understanding the approach. For each spectrum of the average Doppler spectrograms, the frequency of the dominant spectral peak (F1) was evaluated. Using the estimate of the threshold level, the corresponding bandwidth (BW1) of that peak was determined by finding two successive frequency samples with an amplitude lower than that of the threshold on each side of F1. Another spectral peak (F2) was evaluated in the frequency range excluding BW1 and its bandwidth (BW2) extracted in the same way. The boundaries of the spectral envelope were then associated to the minimal and maximal frequency values of the peak having the widest bandwidth. For the Maximal Background Noise Threshold Crossing Method, the same algorithm was used but the maximal amplitude of the statistical distribution function of the background noise was selected as the threshold level instead of a multiple of $\hat{N}_0$ as used with the Modified Threshold Crossing Method.

Improvements of the Hybrid method. No modification of the Hybrid method was performed to estimate the maximal Doppler frequency contours. However, the following improvements were added to the algorithm to immunize it from the high amplitude low-frequency vibrations in the estimation of the minimal frequency contours. The geometric interpretation of the proposed iterative approach evaluated on the negative portion of the spectrogram is illustrated in Fig. 3.

An intersection between the integrated Doppler power spectrum and the straight line originating at the frequency sample corresponding to the cutoff frequency of the wall filter was first searched by solving the following equation:

$$I(\hat{F}\mathrm{min}) = I(-F\mathrm{WALL}) - K\,\hat{N}_0(F\mathrm{WALL} + \hat{F}\mathrm{min}), \tag{2}$$

where $\hat{F}$min is the minimal frequency of the spectrum and FWALL the absolute value of the cutoff frequency of the Wall filter. The estimate of Fmin is given by the highest frequency (in absolute value) that satisfies eqn (2).

If no crossing intersection was found at this first step of the iterative procedure, the frequency of the

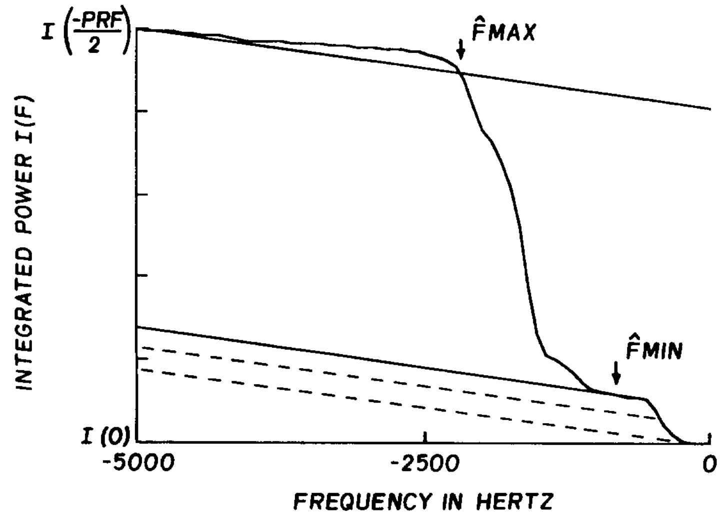

Fig. 3. Geometric interpretation of the Hybrid method. The minimal ($\hat{F}$min) and maximal ($\hat{F}$max) Doppler frequencies are defined by the intersection between the straight lines and the integrated power spectrum. The frequency of the wall filter used in this example was 400 Hz and PRF/2 was 5000 Hz.

starting point of the straight line was moved to the next sample of the $I(f)$ function (*i.e.*, the sample corresponding to $-F$WALL minus one sample). This procedure was repeated until a crossing intersection was found or until the frequency of the starting point of the straight line reached $\hat{F}$max. If no crossing intersection was found at the end of this iterative procedure, $\hat{F}$min was fixed at 0 Hz.

Variability in the shape of the spectral envelopes

To quantify the variability of the spectral envelopes, the Discrete-Fourier representation of the systolic minimal and maximal frequency contours of each spectrogram was evaluated. The ratio in percent of the integrated amplitude of the spectral harmonics described in the following equation was used as an index of variability (IVAR):

$$IVAR = 100 \times \frac{\sum_i X(i)}{\sum_j X(j)} \qquad \begin{array}{r} NDFT/4 < i \leq NDFT/2 \\ 0 < j \leq NDFT/2 \end{array} \qquad (3)$$

where $X(i)$ and $X(j)$ are the amplitude of the discrete Fourier coefficients and $NDFT$ the number of samples of the systolic frequency contours. The same equation was used for $NDFT$ even or odd. A low value of this ratio means that the frequency contour is very smooth while a higher value corresponds to a more erratic contour. To evaluate the influence of the threshold levels on the variability of minimal and maximal frequency contours, values of the index of variability were computed by varying the threshold levels between 1 $\hat{N}_0$ and 20 $\hat{N}_0$ for the Modified Threshold Crossing Method, and parameter K between 0.5 and 10.0 in eqn (1) and eqn (2) for the Hybrid method.

An additional study was performed to assess the sensitivity of the index of variability. Two waveforms having a profile which can be associated to the systolic contours of Doppler spectrograms were simulated. These are the Blackman (Oppenheim and Schafer 1975) and the sine-cosine windows. The number of samples of each window was chosen at 70, which corresponds approximately to the number of samples included in the systolic minimal and maximal frequency contours of Doppler spectrograms. The proposed index was then computed on these windows after adding −25, −20, −15, −10, and −5 dB of random noise. The difference between the index values for each increment of 5 dB was computed on both windows and averaged. The mean value in percent/dB was used to assess the sensitivity of the index of variability. Figure 4 presents the

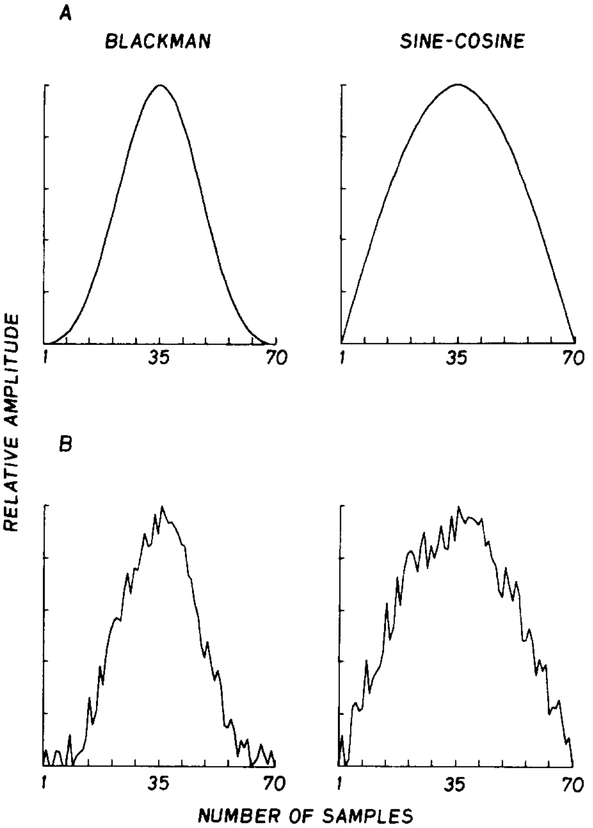

Fig. 4. Blackman and sine-cosine windows used to simulate the systolic frequency contours of Doppler spectrograms. Panel A represents the original windows and Panel B shows the same windows after adding −20 dB of random noise.

Blackman and the sine-cosine windows contaminated by −20 dB of random noise.

Diagnostic value of the spectral parameters

The diagnostic value of the spectral parameters to detect patients with a stenotic aortic valve was estimated with a pattern recognition Gaussian Bayes model (Tou and Gonzalez 1974). The diagnostic accuracy of SEA and SVI was assessed by comparison with the results obtained from the hemodynamic examination and was expressed in term of percentage of correct classifications, sensitivity, and specificity (Feinstein 1977). The percentage of correct classifications of a test is the proportion of the patients who are correctly diagnosed. The sensitivity is the proportion of the patients with aortic valve stenosis who have a positive test while the specificity is the proportion of the patients without aortic pressure gradient who have a negative test.

The basic approach of the Bayes classifier is to find a discriminant function that optimizes the separability of the two classes of patients by minimizing the probability of misclassification. A loss matrix can be used with this classifier to specify the cost associated with each decision. For a two class decision rule, the lost matrix **L** is defined by the elements L_{11}, L_{12}, L_{21}, and L_{22}, where L_{11} and L_{22} are respectively the cost associated to a good classification of the patients without and with aortic pressure gradient. The element L_{12} is the cost associated to a normal patient classified as abnormal while element L_{21} is the cost associated to an abnormal patient classified as normal. A Receiver Operating Curve (ROC) was plotted to describe the relation between the sensitivity and specificity of the spectral parameters (McNeil et al. 1975; Metz 1978). This curve was obtained by varying independently between 0.1 and 0.9 elements L_{12} and L_{21} of the loss matrix. The other elements of the loss matrix were set at 0 for this analysis.

The leave-one-out method (Toussaint 1974) was used to estimate the probability of misclassification of the classifier. In this method, the training set is composed of the complete patient population minus one. This training set is used to design the classifier and the isolated patient is then classified. The procedure is repeated by extracting one patient at a time until all patients have been classified individually. The performance of the classifier is then evaluated by expressing the number of correct classifications in percentage of the total number of patients. Since the leave-one-out method uses almost all of the data to classify one sample at a time, its bias is small (Toussaint 1974). However, the variance of this method can be important and cannot be estimated with precision.

In the present study, the consequence of modifying the threshold levels of the MTCM and the Hybrid method on the percentage of correct classifications of each spectral parameters was investigated. A loss matrix defined by the following elements was used in this specific analysis: $L_{11} = L_{22} = 0$, and $L_{12} = L_{21} = 1$.

3. RESULTS

According to the hemodynamic investigations, 23 patients had no aortic pressure gradient and 25 had average maximal and mean pressure gradients of 81 ± 38 mmHg (mean ± standard deviation, range of 7 to 150 mmHg) and 60 ± 29 mmHg (range of 4 to 120 mmHg), respectively. In the group of patients with no aortic pressure gradient, 4 had minimal-to-mild and 3 had moderate-to-severe aortic regurgitation. The mean age of patients included in this group was 56 ± 12 years (range of 32 to 77 years). In the group of patients with aortic pressure gradient, 15 had minimal-to-mild and 8 had moderate-to-severe aortic insufficiency. The mean age of that group was 65 ± 12 years (range of 35 to 81 years). No statistical difference was found between the cardiac output measured in both groups.

Coefficient of skewness and coefficient of variation used to estimate the background noise

Visual inspection of each average spectrogram showed that 16 presented frequency aliasing. Five spectrograms had frequency aliasing on a large portion of the cardiac cycle which was generally attributed to diastolic aortic regurgitation and eleven had frequency aliasing detected only on some specific spectrum of the spectrogram. The mean values of the coefficient of skewness and of the coefficient of variation of the statistical distribution of the background noise computed on these 16 spectrograms were 5.0 ± 2.1 (range of 2.2 to 9.2) and 151 ± 53% (range of 98 to 263%), respectively. The same statistical parameters estimated on the spectrograms having no frequency aliasing were 2.5 ± 2.0 (range of 0.9 to 7.9) and 70 ± 24% (range of 52 to 145%), respectively. The reference thresholds used to eliminate samples containing blood flow signals were set at 2.5 for the coefficient of skewness and at 70% for the coefficient of variation.

Variability in the shape of the spectral envelopes

The values of the index of variability computed on the Blackman and sine-cosine windows after adding different levels of random noise are presented in Table 1. As shown, the differences in the values of the index computed for each increment of 5 dB are very similar for both windows. Mean values of 6% and 6.5% were obtained, respectively, for the Blackman and the sine-cosine windows. The sensitivity of the index of variability was then estimated at 1.25%/dB of background noise.

The index of variability of the systolic maximal and minimal frequency contours of Doppler spectrograms was computed for the 48 patients. Only the frequency contours corresponding to the negative frequencies of the Doppler spectrograms were analyzed. This portion of the spectrogram corresponds to blood flow moving toward the aorta. Table 2 shows the results obtained with a threshold level of 8 $\hat{N}_0$ for the Modified Threshold Crossing Method, and with a

Table 1. Index of variability computed on the Blackman and sine-cosine windows for different levels of signal-to-noise ratio in dB.

	5 dB	10 dB	15 dB	20 dB	25 dB
Blackman	36%	30%	24%	18%	12%
Sine-cosine	41%	37%	31%	23%	16%

Table 2. Index of variability of the systolic maximal ($\hat{F}$max) and minimal ($\hat{F}$min) frequency contours of average Doppler spectrograms. These indices were evaluated for the Modified Threshold Crossing Method (MTCM), the Maximal Background Noise Threshold Crossing Method (MBNTCM), and the Hybrid method. Threshold level of 8 $\hat{N}_0$ was used for the MTCM and parameter K of eqns (1) and (2) was chosen at 3 for the Hybrid method. $\hat{N}_0$ represents the estimated mean amplitude of the Doppler background noise.

	MTCM	MBNTCM	Hybrid
$\hat{F}$max	26 ± 11%	25 ± 10%	22 ± 8%
$\hat{F}$min	32 ± 8%	33 ± 9%	38 ± 9%

threshold level of 3 (parameter K of equations 1 and 2) for the Hybrid method. These threshold levels were found to be optimal by Mo et al. (1988) for a S/N ratio of the simulated CW Doppler spectrogram ranging between 5 and 13 dB. Spectral envelopes of the spectrogram of Fig. 1 obtained with the three algorithms are also presented in Fig. 5 for visual comparison.

As shown in this Table, the index of variability of the MTCM and the MBNTCM is quite similar to estimate the maximal frequency contours. However, based on a one-way analysis of variance (ANOVA) with repeated measurements, the variability of the Hybrid method is statistically different from that of the MTCM ($p = 0.0005$) and that of the MBNTCM ($p = 0.0045$). Using the sensitivity of this index (1.25%/dB), the S/N ratio of the maximal frequency contours estimated with the Hybrid algorithm is approximately 2.4 dB higher than that obtained with the MBNTCM and 3.2 dB higher than that obtained with the MTCM. The variability of the minimal frequency contours estimated with the Hybrid method is also statistically different from the results obtained with the other algorithms ($p = 0.0001$ for the MTCM and $p = 0.0037$ for the MBNTCM). The S/N ratio of this algorithm is approximately 4 dB lower than that of the other methods. In addition, it is clearly demonstrated in Table 2 that the variability of minimal frequency contours is higher than that of maximal frequency contours for all three algorithms.

Figure 6 describes the influence of the threshold levels for the Modified Threshold Crossing and the Hybrid methods on the index of variability. As expected, the variability of $\hat{F}$min and $\hat{F}$max estimated with both algorithms is maximal for low threshold levels. It decreases rapidly as the threshold level increases to reach a local minimum for $\hat{F}$max and a plateau for $\hat{F}$min. The local minimum of the maximal frequency contour estimated with the MTCM is between 4 $\hat{N}_0$ and 5 $\hat{N}_0$ while that of the Hybrid method is found for $K = 3$. Above the local minimum, the variability of $\hat{F}$max increases for both algorithms with increasing threshold levels. The higher variability of minimal frequency contours compared to that of maximal frequency contours is also seen in this figure.

Discriminating property of the spectral envelope area and the systolic velocity integral

The discriminating property of the spectral envelope area (SEA) and the systolic velocity integral (SVI) to separate patients having a stenotic aortic valve from patients with no aortic pressure gradient was expressed in terms of correct classifications and was evaluated for different threshold levels. Results are presented in Tables 3 and 4 for the Modified Threshold Crossing Method and the Hybrid method, respectively. Threshold levels varying between 4 $\hat{N}_0$

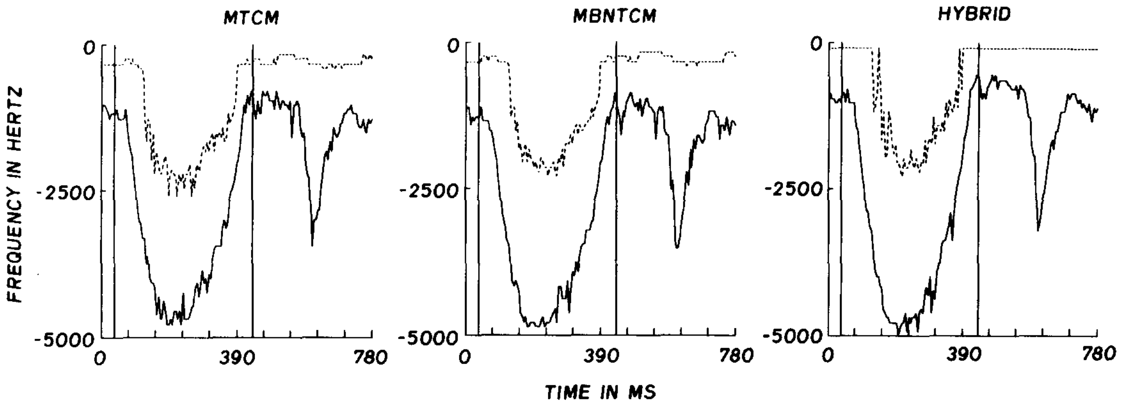

Fig. 5. Spectral envelopes estimated with the Modified Threshold Crossing Method (MTCM), the Maximal Background Noise Threshold Crossing Method (MBNTCM), and the Hybrid method. The vertical lines which correspond to the R wave of the ECG and the beginning of the second heart sound of the phonocardiogram are used to represent the systolic period.

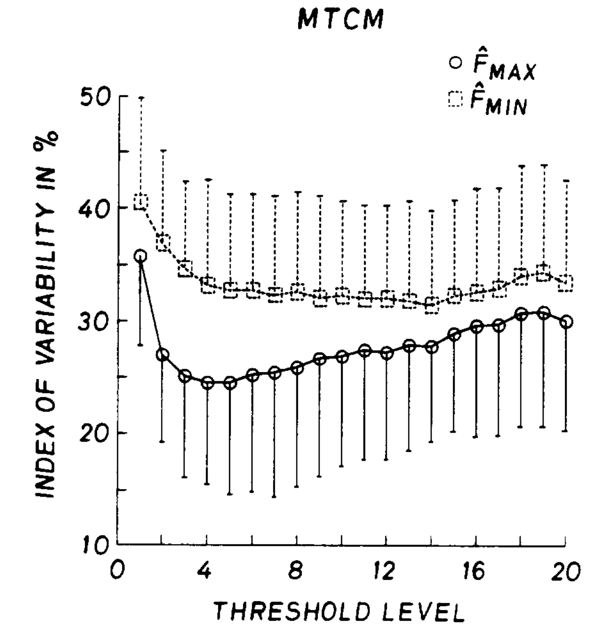

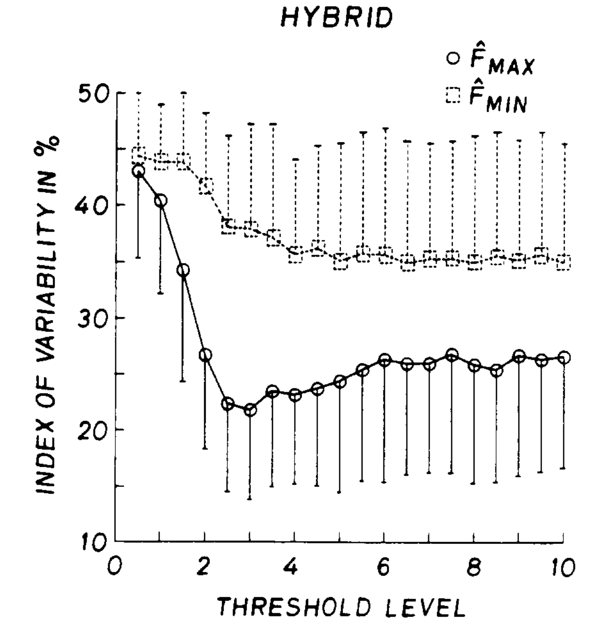

Fig. 6. Influence of the threshold levels on the variability of minimal ($\hat{F}$min) and maximal ($\hat{F}$max) frequency contours. Values of the index of variability were computed by varying the threshold levels between 1 $\hat{N}_0$ and 20 $\hat{N}_0$ for the Modified Threshold Crossing Method (MTCM), and between 0.5 and 10 (parameter K of eqns 1 and 2) for the Hybrid method. The vertical lines represent the standard deviation of the measurements.

and 11 $\hat{N}_0$ were used for the MTCM, and parameter K varying between 3 and 4.5 was used for the Hybrid method. The minimal threshold used for both algorithms corresponds to that providing the minimal variability of $\hat{F}$max. On the other hand, values of 11 $\hat{N}_0$ and $K = 4.5$ are the threshold setting proposed by Mo et al. (1988) for a S/N ratio of CW Doppler spectrogram varying between 13 and 20 dB.

For the MTCM, the percentage of correct classifications obtained with SEA varied between 65% and 71% while that obtained with SVI varied between 54% and 61%. The percentage of correct classifications obtained with SEA estimated with the Hybrid method varied between 63% and 65%. Varying the threshold level did not modify the percentage of correct classifications (67%) obtained with SVI. The best result of SEA was obtained with the MTCM using a threshold level of 8 $\hat{N}_0$ or 9 $\hat{N}_0$ while that of SVI obtained with the Hybrid method was shown to be independent of the threshold level.

To determine the best results that could be reached with the MTCM, the MBNTCM, and the Hybrid method, a Receiver Operating Curve analysis was performed. Threshold levels of 8 $\hat{N}_0$ and parameter $K = 3$ were used for the MTCM and the Hybrid method, respectively. Results are presented in Fig. 7. The black circles and rectangles shown in this figure are the results obtained with a loss matrix defined by the following elements: $L_{11} = L_{22} = 0$, and $L_{12} = L_{21}$

Table 3. Influence of the threshold levels of the Modified Threshold Crossing Method on the percentage of correct classifications (CC) found with the spectral envelope area (SEA) and the systolic velocity integral (SVI). The threshold levels were varied between 4 $\hat{N}_0$ and 11 $\hat{N}_0$, where $\hat{N}_0$ represents the estimated mean amplitude of the Doppler background noise.

Threshold	CC of SEA	CC of SVI
4 $\hat{N}_0$	65%	61%
5 $\hat{N}_0$	67%	61%
6 $\hat{N}_0$	69%	57%
7 $\hat{N}_0$	67%	54%
8 $\hat{N}_0$	71%	54%
9 $\hat{N}_0$	71%	54%
10 $\hat{N}_0$	69%	54%
11 $\hat{N}_0$	69%	54%

Table 4. Influence of the threshold levels of the Hybrid method on the percentage of correct classifications (CC) found with the spectral envelope area (SEA) and the systolic velocity integral (SVI). The threshold parameters K of eqns (1) and (2) were varied between 3 and 4.5.

Threshold	CC of SEA	CC of SVI
3.0	65%	67%
3.5	63%	67%
4.0	63%	67%
4.5	65%	67%

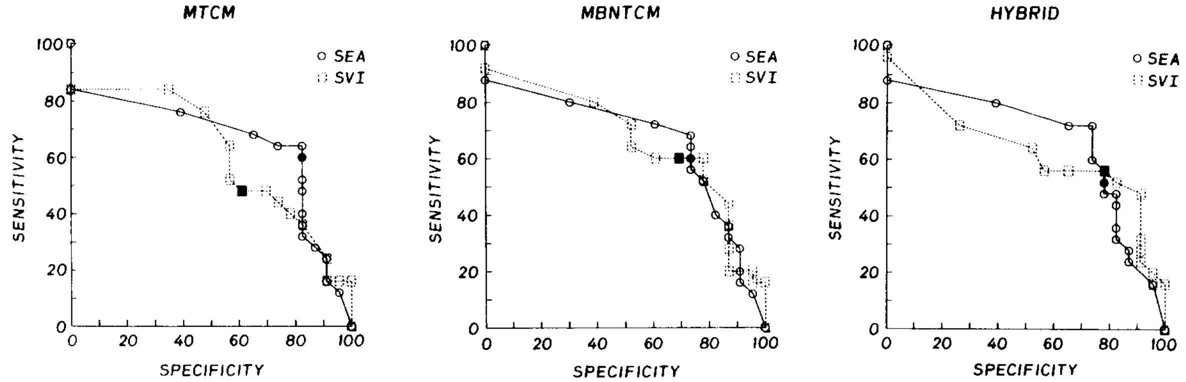

Fig. 7. Receiver Operating Curves of the spectral envelope area (SEA) and the systolic velocity integral (SVI). Results are presented for the Modified Threshold Crossing Method (MTCM), the Maximal Background Noise Threshold Crossing Method (MBNTCM), and the Hybrid method. Black circles and rectangles are the results obtained with a loss matrix defined by the following elements: $L_{11} = L_{22} = 0$, and $L_{12} = L_{21} = 1$. The sensitivity and specificity are expressed in percent.

= 1. The combination of the sensitivity and specificity that corresponds to the higher percentage of correct classifications was chosen to assess the discriminating properties of the spectral parameters. Based on the results shown in Table 5, the discriminating properties of the spectral envelope area (SEA) seem to be slightly better than those obtained with the systolic velocity integral (SVI) for all algorithms.

4. DISCUSSION

Averaging of Doppler spectrograms

As reported in the Method section, an ensemble average of the power spectrograms computed on 5 cardiac cycles was taken to reduce the variability of the spectral representation. Averaging of spectral lines over successive heartbeats had been previously suggested by Greene et al. (1982) to handle spectra of arterial flow. However, no criterion was defined in the study of Greene et al. to select the optimal number of cardiac cycles that should be averaged to reduce, by a given amount, the variability of the Doppler spectrograms. The evaluation of such criterion and information on beat-to-beat variations of the spectrograms could be the object of an interesting paper.

Table 5. Percentage of correct classifications (CC), sensitivity and specificity obtained with the spectral envelope area (SEA) and the systolic velocity integral (SVI) estimated with the Modified Threshold Crossing Method (MTCM), the Maximal Background Noise Threshold Crossing Method (MBNTCM), and the Hybrid method. Threshold level of 8 $\hat{N}_0$ was used for the MTCM and parameter K of eqns (1) and (2) was chosen at 3 for the Hybrid method. $\hat{N}_0$ represents the estimated mean amplitude of the Doppler background noise.

		CC	Sensitivity	Specificity
SEA	MTCM	73%	64%	83%
	MBNTCM	71%	68%	74%
	Hybrid	73%	72%	74%
SVI	MTCM	62%	76%	48%
	MBNTCM	69%	60%	78%
	Hybrid	69%	48%	91%

Effects of the background noise threshold setting on the variability of the spectral contours

Estimating the background noise with a threshold setting that is too low will generally increase the variability in the shape of the spectral contours. This was clearly demonstrated in Fig. 6. It is interesting to note from this figure that the threshold value which minimizes the variability of maximal frequency contours of PW Doppler signals estimated with the Hybrid method corresponds exactly to the threshold setting proposed by Mo et al. (1988) for a S/N ratio of CW Doppler spectrogram ranging between 5 and 13 dB. For the Modified Threshold Crossing Method, the threshold setting proposed by Mo et al. (1988) was 8 $\hat{N}_0$ for the same range of S/N ratios. In the present study, threshold values of 4 $\hat{N}_0$ or 5 $\hat{N}_0$ minimize the variability of maximal frequency contours. However, as shown in Fig. 6, the variability of $\hat{F}$max for a threshold of 8 $\hat{N}_0$ is only 1.4% (or 1.1 dB) higher than the results obtained for a threshold of 4 $\hat{N}_0$ or 5 $\hat{N}_0$. Moreover, the variability of $\hat{F}$min continues to decrease above 5 $\hat{N}_0$. Based on these results, the threshold setting of 8 $\hat{N}_0$ proposed by Mo et al. (1988) appears to be a good compromise between minimization of the variability of both $\hat{F}$max and $\hat{F}$min.

The variability in the shape of the minimal frequency contours of each patient was almost always higher than that of the maximal frequency contours for all algorithms and for all threshold settings. This strongly suggests that the background noise is not constant as a function of frequency (or not a white Gaussian process). Indeed, a colored background noise (pink noise for instance) having an amplitude decreasing with frequency (in absolute value) would probably be a better model to explain the higher variability in the shape of minimal frequency contours. Another explanation could be that the amplitude of Doppler blood flow signals increases with frequency (in absolute value).

Effects of the background noise threshold setting on the diagnostic value of the spectral parameters

A bad threshold setting could have the following consequences on the accuracy of the spectral envelope: A high threshold will reduce the area of the spectral envelope while a low threshold will increase its value. Moreover, because the maximal frequency contours are limited to PRF/2 and −PRF/2, saturation of the envelope could also be obtained for a threshold setting that is too low. A complementary study was then performed to evaluate the effects of using a threshold setting that is too low and one that is too high, on the diagnostic value of SEA and SVI. Specifically, the percentage of correct classifications for the Bayes model was evaluated for threshold settings of 1 $\hat{N}_0$ and 20 $\hat{N}_0$ for the MTCM, and for threshold settings of 0.5 and 10 (parameter K of equation 1 and 2) for the Hybrid method.

For the low threshold values, the percentage of correct classifications of SEA estimated with the MTCM and the Hybrid method was, respectively, 56% and 52% which is significantly lower than the results presented in Tables 3 and 4. Similar observation (46% of correct classifications) was noted for SVI estimated with the Hybrid method. On the other hand, SVI evaluated with the MTCM gave a similar result (60% of correct classifications) than those reported in Table 3.

For the high threshold values, the percentage of correct classifications of SEA and SVI estimated with the MTCM was not significantly different than the results of Table 3. Values of 65% and 61% were respectively obtained. The percentage of correct classifications of SEA and SVI evaluated with the Hybrid method was, respectively, 63% and 59%. The diagnostic value of SEA is similar to that reported in Table 4. However, the percentage of correct classifications of 59% obtained with SVI is significantly lower than the value of 67% shown in Table 4. Based on these results, it appears that a threshold setting which is too low has a greater influence than one which is too high. The worst results were generally obtained for a threshold of 1 $\hat{N}_0$ for the MTCM and for K equals 0.5 for the Hybrid method. As shown in Fig. 6, these thresholds correspond also to the higher variability of minimal and maximal frequency contours for both algorithms.

Significance of the diagnostic results

The results concerning the values of SEA could not directly be compared to the results of Richards et al. (1983) which were obtained from Doppler signals recorded approximately 4 cm above the aortic valve. In addition, areas were computed by planimetry and had not the same number of spectral lines. In the present study, the number of spectral lines was determined by the duration and time overlap between each Hanning window used to compute the Doppler spectrogram. Typical values of SEA estimated with the Modified Threshold Crossing Method (threshold of 8 $\hat{N}_0$ are 68 ± 38 kHz for the group of patients having no aortic pressure gradient, and 107 ± 54 kHz for the group of patients with a stenotic aortic valve.

The best discriminating performance obtained with the spectral envelope area was 73% of correct classifications while that obtained with the systolic velocity integral was 69% of correct classifications. At first glance, these results are not very impressive. However, related to the continuity equation (Otto et al. 1986; Zoghbi et al. 1986; Oh et al. 1988), they could find an interesting application. The rationale behind the continuity equation is as follow: With flow remaining constant across the stenotic valve, the ratio of the cross-sectional areas of the aortic root and of the aortic stenotic orifice should be inversely proportional to the ratio of the respective mean or maximal instantaneous velocities. The mean velocities are generally obtained by computing the systolic velocity integral of the PW Doppler spectrogram recorded below the aortic valve, and of the CW spectrogram recorded in the aortic jet. Because the discriminating properties of the spectral envelope area are better than those obtained with the systolic velocity integral, a better estimate of the mean instantaneous velocity could probably be obtained by using the spectral envelope area instead of the systolic velocity integral.

In the present study, we assumed that the probability density function of the spectral parameters was Gaussian. A Gaussian Bayes classifier was then used to evaluate the diagnostic performance of SEA and SVI. As a complementary study, we have estimated the histogram distribution of SEA and SVI for each group of patients and for each method (MTCM, MBNTCM, and Hybrid method). A threshold level of 8 $\hat{N}_0$ and 3 was respectively used for the MTCM and the Hybrid method. A Shapiro-Wilk statistic test (available in SAS statistical package) was used to evaluate the hypothesis of having Gaussian distributions. In the group of patients having no aortic pressure gradient, the hypothesis of having Gaussian distributions was not rejected for both SEA and SVI ($p > 0.05$). The p-values were 0.11, 0.08, and 0.09 for SEA estimated with the MTCM, MBNTCM and Hybrid method, respectively. Values of 0.44, 0.30, and 0.20 were measured for SVI estimated with the three algorithms. In the group of patients with aortic valve stenosis, we concluded in a same way. The p-values were 0.55, 0.16, and 0.22 for SEA computed with the MTCM, MBNTCM, and Hybrid method, respectively. Values of 0.17, 0.13, and 0.50 were obtained for SVI. Based on these results, the use of a Gaussian Bayes classifier was justified to estimate the percentage of correct classifications of each spectral parameter.

5. CONCLUSION

The variability in the shape of minimal and maximal frequency contours of Doppler spectrograms estimated with the Modified Threshold Crossing Method and the Hybrid method was evaluated in 48 patients, as a function of the threshold level used in each algorithm. The variability of minimal and maximal frequency contours was found to be maximal for low threshold levels. That of minimal frequency contours was also shown to be less influenced by the threshold setting. Moreover, the variability of minimal frequency contours was always higher than that of maximal frequency contours for all algorithms and all threshold settings.

A new algorithm was also proposed in the present study to estimate minimal and maximal frequency contours. This algorithm is the Maximal Background Noise Threshold Crossing Method. The main advantage of this algorithm is that no threshold setting is needed. Moreover, the diagnostic performance of SEA and SVI estimated with this algorithm was, respectively, 71% and 69% of correct classifications which is similar to the best results reported with the other algorithms (73% of correct classifications for SEA and 69% of correct classifications for SVI).

An important finding of this study is the method proposed to estimate the background noise of Doppler spectrograms. The effectiveness of the approach used to eliminate Doppler blood flow signals in the computation of the background noise was appreciated by visual inspection of the frequency contours. Although the background noise is probably not white and Gaussian, its estimate was satisfactory for almost all patients. Without using this new method, all algorithms would overestimate the background noise and consequently the corresponding threshold level in the presence of frequency aliasing.

A last comment concerning the estimation of the background noise is that our method can be used for both PW and CW Doppler spectrograms. Instead of using the mean amplitude of samples localized close to ±PRF/2, as used for PW Doppler analysis, the mean amplitude of samples found at the extinction frequency of the low-pass filtering of the signal or at the sampling frequency divided by two could be used for the CW Doppler analysis. Finally, as reported in the Method section, another important finding of the present study is the approach proposed to reduce the influence of high amplitude low-frequency vibrations in the computation of the minimal frequency contours.

Acknowledgment—This research was supported by the Natural Sciences and Engineering Research Council of Canada, the Fonds de la Recherche en Santé du Québec, the Canadian Heart Foundation and the Monat Foundation, Université de Montréal.

The authors gratefully acknowledge the contributions of the following persons: Dr. George Honos, resident V in cardiology at the Hôtel-Dieu de Montréal Hospital, Drs. Michel Jarry, Alain Solignac, Richard Essiambre, and Denis-Carl Phaneuf of the Cardiology Division of the Hôtel-Dieu de Montréal Hospital for their participation in the collection of the hemodynamic and Doppler data. Acknowledgments are also addressed to Mrs. Michel Blanchard and Louis Allard for developing, respectively, the Bayes pattern recognition program and the patient data base structure used in this study, and Mr. François Bellavance for his suggestions about the statistical aspects of the paper.

REFERENCES

Berger, M.; Berdoff, R. L.; Gallerstein, P. E.; Goldberg, E. Evaluation of aortic stenosis by continuous wave Doppler ultrasound. J. Am. Coll. Cardiol. 3:150–156; 1984.

Cannon, S. R.; Richards, K. L.; Rollwitz, W. T. Digital Fourier techniques in the diagnosis and quantification of aortic stenosis with pulsed-Doppler echocardiography. J. Clin. Ultrasound 10:101–107; 1982.

Cannon, S. R.; Richards, K. L.; Morgann, R. G. Comparison of Doppler echocardiographic peak frequency and turbulence parameters in the quantification of aortic stenosis in a pulsating flow model. Circulation 71:129–135; 1985.

Currie, P. J.; Seward, J. B.; Reeder, G. S.; Vlietstra, R. E.; Bresnahan, D. R.; Bresnahan, J. F.; Smith, H. C.; Hagler, D. J.; Tajik, A. J. Continuous-wave Doppler echocardiographic assessment of severity of calcific aortic stenosis: a simultaneous Doppler-catheter correlative study in 100 adult patients. Circulation 71:1162–1169; 1985.

D'Alessio, T. "Objective" algorithm for maximum frequency estimation in Doppler spectral analysers. Med. Biol. Eng. Comput. 23:63–68; 1985.

Fan, P.-H.; Kapur, K. K.; Nanda, N. C. Color-guided Doppler echocardiographic assessment of aortic valve stenosis. J. Am. Coll. Cardiol. 12:441–449; 1988.

Feinstein, A. F. On the sensitivity, specificity, and discrimination of diagnostic tests. In: Clinical biostatistics. St-Louis: C. V. Mosby; 1977:214–226.

Greene, F. M. Jr.; Beach, K.; Strandness, D. E. Jr.; Fell, G.; Phillips, D. J. Computer based pattern recognition of carotid arterial disease using pulsed Doppler ultrasound. Ultrasound Med. Biol. 8:161–176; 1982.

Grossman, W. Cardiac catheterization and angiography (3rd ed.). Philadelphia: Lea and Febiger; 1986.

Harward, T. R. S.; Bernstein, E. F.; Fronek, A. The value of power frequency spectrum analysis in the identification of aortoiliac artery disease. J. Vasc. Surg. 5:803–813; 1987.

Hatle, L.; Angelsen, B. A.; Tromsdal, A. Non-invasive assessment of aortic stenosis by Doppler ultrasound. Br. Heart J. 43:284–292; 1980.

Heringa, A.; Alsters, J.; Hopman, J.; van Dam, I.; Daniels, O. Computer processing of cardiac Doppler signals. Med. Biol. Eng. Comput. 26:147–152; 1988.

Hoeks, A. P. G.; Ruissen, C. J.; Hick, P.; Reneman, R. S. Methods to evaluate the sample volume of pulsed Doppler systems. Ultrasound Med. Biol. 10:427–434; 1984.

McNeil, B. J.; Keeler, E.; Adelstein, S. J. Primer on certain elements of medical decision making. N. Engl. J. Med. 293:211–215; 1975.

Metz, C. E. Basic principles of ROC analysis. Seminars in Nucl. Med. 8:283–298; 1978.

Mo, L. Y. L.; Yun, L. C. M.; Cobbold, R. S. C. Comparison of four digital maximum frequency estimators for Doppler ultrasound. Ultrasound Med. Biol. 14:355–363; 1988.

Oh, J. K.; Taliercio, C. P.; Holmes, D. R. Jr.; Reeder, G. S.; Bailey, K. R.; Seward, J. B.; Tajik, A. J. Prediction of the severity of aortic stenosis by Doppler aortic valve area determination: prospective Doppler-catheterization correlation in 100 patients. J. Am. Coll. Cardiol. 11:1227–1234; 1988.

Oppenheim, A. V.; Schafer, R. W. Digital signal processing. Englewood Cliffs, NJ: Prentice-Hall, Inc.; 1975.

Otto, C. M.; Pearlman, A. S.; Comess, K. A.; Reamer, R. P.; Janko, C. L.; Huntsman, L. L. Determination of the stenotic aortic valve area in adults using Doppler echocardiography. J. Am. Coll. Cardiol. 7:509–517; 1986.

Panidis, I. P.; Mintz, G. S.; Ross, J. Value and limitations of Doppler ultrasound in the evaluation of aortic stenosis: A statistical analysis of 70 consecutive patients. Am. Heart J. 112:150–158; 1986.

Penn, I. M.; Dumesnil, J. G. A new and simple method to measure maximal aortic valve pressure gradients by Doppler echocardiography. Am. J. Cardiol. 61:382–385; 1988.

Portnoff, M. R. Time-frequency representation of digital signals and systems based on short-time Fourier analysis. IEEE Trans. Acoust. Speech Signal Process. ASSP-28:55–68; 1980.

Richards, K. L.; Cannon, S. R.; Crawford, M. H.; Sorensen, S. G. Noninvasive diagnosis of aortic and mitral valve disease with pulsed-Doppler spectral analysis. Am. J. Cardiol. 51:1122–1127; 1983.

Stamm, R. B.; Martin, R. P. Quantification of pressure gradients across stenotic valves by Doppler ultrasound. J. Am. Coll. Cardiol. 2:707–718; 1983.

Tou, J. T.; Gonzalez, R. C. Pattern recognition principles. Reading, MA: Addison-Wesley; 1974.

Toussaint, G. T. Bibliography on estimation of misclassification. IEEE Trans. Info. Theory IT-20:472–479; 1974.

van Merode, T.; Hick, P.; Hoeks, A. P. G.; Reneman, R. S. Limitations of Doppler spectral broadening in the early detection of carotid artery disease due to the size of the sample volume. Ultrasound Med. Biol. 9:581–586; 1983.

Zoghbi, W. A.; Farmer, K. L.; Soto, J. G.; Nelson, J. G.; Quinones, M. A. Accurate noninvasive quantification of stenotic aortic valve area by Doppler echocardiography. Circulation 73:452–459; 1986.

Zoghbi, W. A. Echocardiographic and Doppler ultrasonic evaluation of valvular aortic stenosis. Echocardiography, A Review of Cardiovascular Ultrasound 5:23–38; 1988.